https://doi.org/10.33472/AFJBS.6.9.2024.4841-4852

African Journal of Biological Sciences

Journal homepage: http://www.afjbs.com

Research Paper Open Access

Evaluation of Anti-cancer Efficacy of *Eleaocarpus Ganitrus* (Rudraksha) Bead Mediated Silver Nanoparticles in Mouse Lewis lung carcinoma tumour model

Milind Sagar[1], Prashant Kumar Pandey[1], Shiva Sharma[1], Manisha Rastogi[1]*

[1]School of Biomedical Engineering and Science, Shobhit Institute of Engineering and Technology (NAAC "A" Accredited Deemed to be University), NH-58, Modipuram, Meerut, UP, India

*Corresponding author:

Dr. Manisha Rastogi
Associate Professor
School of Biomedical Engineering and Science,
Shobhit Institute of Engineering and Technology
(NAAC "A" Accredited Deemed to be University),
NH-58, Modipuram, Meerut, UP, India
manisha.rastogi@shobhituniversity.ac.in

Article History
Volume 6, Issue 9, 2024
Received: 23 April 2024
Accepted: 13 June 2024
doi: 10.33472/AFJBS.6.9.2024.4841-4852

Abstract

Cancer is a major worldwide health concern therefore warranting the development of new and effective therapeutic options. The potential anti-cancer capabilities of silver nanoparticles (AgNPs) derived from medicinal plants have garnered significant attention in recent times. the present work aims to evaluate an *in vivo* anti-cancer efficacy in the Mouse Lewis lung carcinoma (LLC1) lung tumour model accompanied with an *in vivo* safe dose selection study in C57BL/6 mice. The safe dose of REMAG for anti-cancer activity was tested at three doses,viz., low (10 mg/kg), mid (30 mg/kg) and high (60 mg/kg) dose in C57BL/6 mice (male and female). The biogenic AgNPs were found to be biocompatible with no abnormal body weightchanges, clinical signs, and gross pathological observations in healthy male and female mice. An excellent tumor inhibition response of 77% was obtained at the selected dose of 50 mg/kgin the LLC1 tumour allograft model. The outcomes propose the promising candidature of synthesized AgNPs for anti-cancer efficacy and future studies are warranted in other cancer cell lines and for its molecular mechanism of actions.

Keywords: Biogenic silver nanoparticles; Rudraksha bead; Biocompatible; Anticancer activity, Tumor inhibition

Introduction

Cancer is still a major global health concern, necessitating the development of novel and efficient treatment approaches. According to the Global Cancer Observatory (GLOBOCAN) estimation, 19.3 million cases of cancer occured worldwide in 2020, with the US and China having top two incidence and India at third place (Sung et al., 2021; Ferlay et al., 2022). For the year 2022, the anticipated crude incidence and prevalence rate of cancer cases in India was 14,61,427 (100.4 per 100,000) with higher prevalence in females (105.4 vs. 95.6 per 100,000). This incidence is expected to reach to 2.08 million cancer cases in India by 2040, according to GLOBOCAN's prediction (Ferlay et al., 2022). There is an urgent need to develop better treatment regimens in addition to the already recommended conventional treatment tactics of radiation, chemotherapy, and surgery due to the growth in cancer incidence. Globally, researchers have been exploring novel approaches to cancer therapy, with a particular emphasis on nanotechnology-driven solutions. A variety of metallic nanoparticles have been created primarily through physical, chemical and biological methods; however silver nanoparticles (AgNPs) synthesized using using plant extract have gained considerable attention (Pallela et al., 2019; Singh et al., 2019; Pirtarighat et al., 2019). This is due to its greater biocompatibility, non-toxicity, environmental friendliness, and economic feasibility. Research showcasing the possible anti-tumor properties of green produced AgNPs utilizing several medicinal plants is increasing (Simon et al., 2023; Wani et al., 2021). Numerous studies showed that biogenic AgNPs have multiple anti-cancer mechanisms of action in various cancer lines, such as cytotoxicity mediated by reactive oxygen species (ROS), changes in the potential of the mitochondrial membrane, cell cycle arrest, and modifications to apoptotic signalling pathways (Chairuangkitti et al., 2013; Banerjee et al., 2017).

Rudraksha (*Elaeocarpus ganitrus roxb*) is a well-known medicinal plant documented for its antimicrobial, anti-cancer, antioxidant, immunomodulatory, anti-hypertensive, anti-depressant, nephroprorotective, anti-diabetic, anti-atherosclerotic, and anti-parkinsonian effects (Rai et al., 2019). Previous research reported that Rudraksha beads are rich in alkaloids, saponins, flavonoids, phenolics, anthocyanins, ascorbic acid, tannins, terpenoids, and 23 mineral elements, which may have potential impact on both synthesis of NPs as well as anti-cancer properties (Sharma et al., 2021). Further, previous research also demonstrated the unique electromagnetic (weak ferromagnetic and dielectric) behavior of Rudraksha beads (Sharma et al., 2019 and 2023). Regarding the environmentally friendly production of AgNPs

from Rudraksha, Dwivedi et al. (2014) investigated the synthesis of nanocomposite using a chitosan matrix and Rudraksha beads mediated AgNPs. The study reported remarkable resistance of nanocomposites to degradation, disintegration, or degeneracy with good anti-microbial and biocompatibility properties. In our recent study, we have extensively characterized the silver nanoparticles prepared from Rudraksha (*Elaeocarpus ganitrus* roxb) beads through UV-Visible Field Emission, Scanning Electron Microscope (FESEM), Transmission Electron Microscope (TEM), X-ray Diffraction (XRD), Energy Dispersive X-ray (EDX), and Fourier Transfer Infrared (FTIR). The study demonstrated the synthesis of spherical AgNPs of approximately 57 nm size with optimum *in vitro* cytotoxicity in three cancer cell lines, human prostate cancer (PC3), human glioblastoma (U87MG), and Mouse Lewis lung carcinoma (LLC1). The study further revealed maximum cytotoxicity in LLC1 cell line with an IC_{50} of 9.7 ± 1.0 µg/mL. (paper accepted). However, *in vivo* studies related to the anti-cancer activity of REMAG has not been reported earlier. Considering the potential *in vitro* cytotoxicity activity of Rudraksha mediated silver nanoparticles (REMAG) in our previous study, the present work aims to evaluate an *in vivo* anti-cancer efficacy in the Mouse Lewis lung carcinoma (LLC1) lung tumour model accompanied with an *in vivo* safe dose selection study in C57BL/6 mice.

Methods

Materials

Rudraksha beads were collected from the repository of Kunwar Shekhar Vijendra Ayurvedic Medical College and Research Center, Shobhit University, Gangoh. $AgNO_3$ and DMSO and 3-(4,5-dimethylthiazol-2-yl)-2,5-diphenyltetrazolium bromide (MTT) were procured from Sigma Aldrich Pvt. Ltd. The mouse Lewis lung carcinoma (LLC1/LL/2, CRL-1642) lines was procured from American Type Culture Collection (ATCC), USA. F12K, EMEM, DMEM, Penicillin/streptomycin and Fetal Bovine serum (FBS) were procured from Gibco. Cisplatin was procured from a pharmacy.

Preparation of aqueous extract of Rudraksha

Collected Rudraksha beads were washed with sterile water and crushed to a coarse powder using regular mixer grinder. About 10 g of powder was added to 100 mL of deionized water, stirred with magnetic stirrer and heated to 80^{o}C for 4 h. The aqueous extract of the bead was obtained by filtering the above mixture using Whatman 41 filter paper under vacuum. The extract was stored in refrigerator at 2-8^{o}C until further use.

Synthesis of biogenic AgNPs

Rudraksha extract mediated silver nanoparticles (REMAG) was carried out by simple reduction process. A 50mL of aqueous 1 mM $AgNO_3$ solution was taken in 100 mL beaker and a 2.5 mL of above synthesized bead extract was added. The solution mixture was heated to 30 min at 65^{o}C and allowed to cool at room temperature. The change in the color of a solution mixture was observed for 12 h, 24 h and 48 h. The solutions were further centrifuged at 15000 × g for 20 min. The centrifugation was repeated twice to get rid of unreacted impurities. The formation of AgNPs was primarily confirmed at each time points using UV-Vis spectrophotometer and characterized by FESEM, TEM, XRD, EDX, and FTIR techniques as described previously.

Animals

Male and female-, 6-8 weeks aged C57BL/6 mice were obtained from in house breeding source of Skanda Life Sciences, Bidadi, Bangalore. Healthy and active mice were selected in the study. Animals were taken care as per the regulations of Committee for Control and Supervision of Experiments on Animals (CCSEA), Government of India. The experimental design was reviewed and approved by the Institutional Animals Ethics Committee under protocol No. IAEC-SLS-2022-066. All the animals were housed in IVC with filter top individually ventilated cages and maintained in sterile environment with daily 12 h light/ 12 h dark cycle, 55 ± 15 % relative humidity and 23 °C ± 3 °C temperature. Animals were given *ad libitum*, autoclaved commercial diet and water.

In vivo safe dose selection and anti-cancer efficacy study

Three dose levels of REMAG- 10, 30 and 60 mg/kg were selected for the identification of safe dose for further anti-cancer activity referring the previous studies (Hassanen et al., 2019). Safe dose was considered as a dose where animals showed less than 10% reduction in body weight with no major changes in clinical signs and no gross pathological observations in vital organs such as brain, lungs, heart, liver, spleen, kidneys and gastrointestinal tract at the time of necropsy. The screening of safe dose was done using 6 mice (3 males and 3 females) per group. For all the dose levels, AgNPs was formulated using DPBS (1x). Control group animals were treated with DPBS (1x). All animals were treated intraperitoneally every alternate day at a dose volume of 10 mL/kg. On the 7th day of the study, all animals were

humanely euthanized. Body weight and clinical signs were noted daily during the experimental period.

% body weight change (% BWC) was calculated considering initial body weight of each animal using following formula:

$$\%\, BWC = (\frac{BW_{dx} - BW_{d0}}{BW_{d0}}) \times 100$$

Where, BW_{dx} - Body weight of day x, BW_{d0}- Body weight of day 0

For *in vivo* anti-cancer study, LLC1 cells were cultured in DMEM containing 10% FBS and 1% Penicillin/streptomycin. Six-to-eight-week aged C57BL/6 mice were subcutaneously implanted with $1x10^6$ LLC1 cells per mouse and monitored for tumor growth. Animals were randomized once tumor attained the optimum range and divided into 6 mice per group with a mean tumor volume of ~115 mm^3 and treatment were initiated. Group 1 and 2 were intraperitoneally treated with DPBS (1x) and AgNPs (50 mg/kg) respectively Q2D x 6 at a dose volume of 10 mL/kg. Tumor was measured using Vernier calliper at every 3rd day during the study period up to 12 days. Tumor volume was calculated from two tumor diameter measurements (length- large diameter; width- short diameter) using the formula:

$$Tumor\ volume\ (mm^3) = \frac{Tumor\ length \times tumor\ width^2}{2}$$

Anti-cancer activity was evaluated as tumor growth inhibition in the REMAG treated group compared to vehicle treated group. The tumor growth inhibition (TGI) was calculated using following formula:

$$\%\, TGI = (1 - \frac{T}{C}) \times 100$$

Where, T- Mean TV of the test group; C- Mean TV of the vehicle control group.

Animals were observed for any visible clinical signs and body weight change of individual animal was also calculated to check the weight loss or gain. The study was terminated on day 12 as tumors from vehicle control group reached tumor humane end point (TV ≥ 1500 mm^3) and all animals were humanely euthanized using CO_2 exposure method, subjected to the gross necropsy.

Statistical Analysis

Statistical analysis for *in vivo* safe dose selection was performed using two-way ANOVA followed by Bonferroni *post hoc* test. The tumor growth profile is represented as tumor volume (Mean ± SD). Significant differences were probed using Student t-test. Probability values *$p < 0.05$, **$p < 0.01$ and ***$p < 0.001$ were considered as significant.

Results and Discussion

This study identified the maximum tolerated dose (MTD) of REMAG and demonstrated its considerable anti-cancer activity in the LLC1 lung tumour model. Our previous study successfully synthesized and characterized the REMAG with the formation of ~ 57 nm spherical AgNPs. The FT-IR outcomes of the study revealed the presence of peaks corresponding to alcohols, phenols, alkanes, and proteins eventually as reducing, capping, and stabilizing agents with benefits both in AgNPs synthesis as well as anti-cancer activity. Further, REMAG showed dose dependent cytotoxicity in all the three tested cell lines (LLC1>U87MG> PC3) with an IC_{50} below 20 µg/mL. These results provided provided strong rationale to assess the anti-cancer efficacy of a selected dose of REMAG in an *in vivo* tumor mouse model using the mouse lung cancer cell line LLC1, where the maximum cytotoxic response was obtained.

Since, no previous study was available to use as a reference dose, this study determined the safe dose of REMAG for anti-cancer activity amongst the three doses, viz., low (10 mg/kg), mid (30 mg/kg) and high (60 mg/kg) dose in C57BL/6 mice (male and female). Changes in body weight, clinical signs, and gross pathological observations post necropsy were recorded. Figure 1 (a) and (b) illustrated the percentage change in body weight demonstrating the gradual body weight gain in male and female mice after REMAG dosing at low (10 mg/kg) and mid (30 mg/kg) doses. While at a high dose (60 mg/kg), transient weight loss was observed in male mice (maximum 1.7 % weight loss on day 4) and females (maximum 5.1 % weight loss on day 5), no significant weight loss was observed except for 60mg/kg dose in the female group. However, changes in % body weight was within the acceptable range of ≥ 10 %. Further, no major changes in clinical signs were noticed at the tested doses. Gross pathological observations were found to be apparently normal without any gross lesions or abnormal appearance in all vital organs, such as the brain, liver, lungs, heart, spleen, kidneys, and GI tract, post-necropsy. Overall, animals at all three tested doses of REMAG were apparently normal with no abnormal clinical observations and were therefore considered tolerable and safe for anti-cancer activity assessment. Nevertheless, a partial lower dose of 50 mg/kg was selected considering the mild weight loss at 60 mg/kg and the possibility of a

longer dosage regimen until the maximum volume of 1500 mm^3 in the control group of the LLC1 tumor allograft study.

Tumor growth profile during REMAG treatment is illustrated in Figure 2. Tumor growth profile revealed that the vehicle control group exhibited progressive tumor growth and the mean tumor volume on day 12 was 1591±154 mm^3. Statistically significant inhibition in tumor growth was observed in the REMAG treated group since day 6 and onwards, with a mean tumor volume of 361±22 mm^3 on day 12 (Table 1). The percentage tumor growth inhibition (% TGI) for REMAG at 50 mg/kg on day 12 was 77%, demonstrating an excellent anti-cancer activity of REMAG (Table 2). The real-time pictures of both groups showing the tumor on day 12 are provided in Figure 3. The photographs evidently showed the efficacy of REAMG in inhibiting tumor growth compared to vehicle control. In addition to the tumor growth profile for test groups, the body weight changes were also noted every 3 days, and the change in % body weights are shown in Figure 4. A gradual body weight increase was observed in both groups. Different physico-chemical variables, specifically the shape and size of the obtained AgNPs can be attributed to the anti-cancer efficacy. Several studies demonstrated size-dependant outcomes on cell viability and oxidative stress generation in different cell lines (Akter et al., 2018). Most of these studies indicated that the smaller the AgNPs, higher the toxicity, however few studies also reported no direct association between size and cytotoxicity (Kaba and Egorova, 2015). It is worth highlighting that while obtaining maximum cytotoxicity over cancer cells is the ultimate goal for any potential anti-cancer agent, the toxicity impact over normal cells should also be ascertained. A study conducted by Cho *et al*. reported the size-dependant acute toxicity of AgNPs, where the smallest size NPs of 10 nm demonstrated high acute toxicity when compared with bigger size NPs of 60 nm and 100 nm with no toxicity (Cho et al., 2018). In our study, selection of biogenic AgNPs with an optimum size of approximately 57 nm obtained at 48 h may be one of the potential reasons for well – tolerated dose at all dosage levels in healthy male and female mice. Further, REMAG is highly biocompatible, which is in accordance with the published evidences that demonstrated lower to no toxicity of biogenic AgNPs when compared between cancer cell lines and normal cells (Morais et al., 2020). The enhanced biocompatibility may also be rendered to the natural phytoconstituents as surface capping for AgNPs. The selective cytotoxicity and vulnerability of cancer cells may also be due to the higher uptake of biogenic AgNPs as a consequence of abnormal metabolism and a higher proliferation rate (Khorrami et al., 2018). The entrance of AgNPs within the cancer cells may also be partially influenced

by the shape of NPs, which are mostly spherical in shape when phytosynthesized, as in the present study (Ratan et al., 2020).

Figures

Figure 1: %Body weight change of male and female mice during REMAG treatment

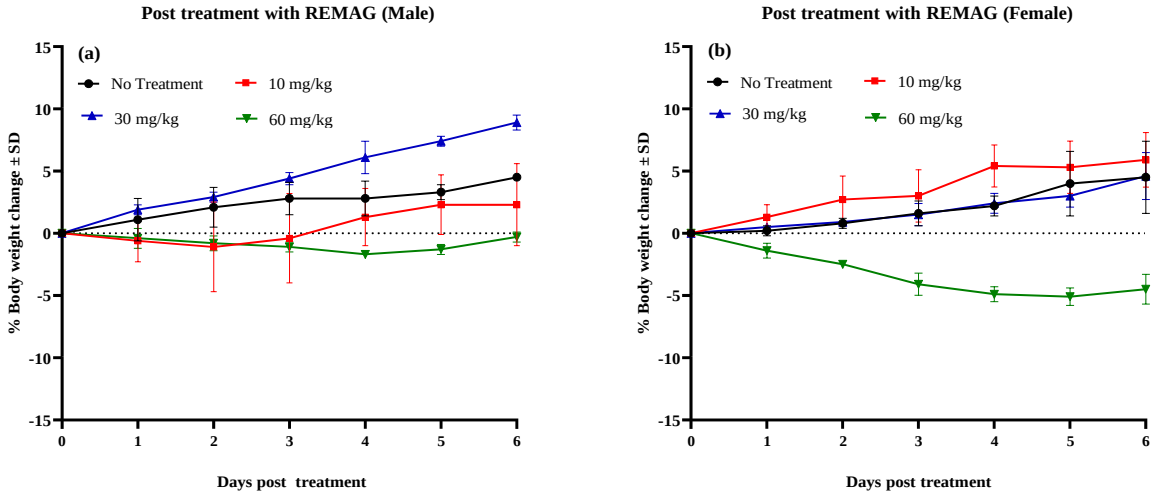

Figure 1: % change in body weights of (a) male and (b) female mice after REMAG treatment. Statistical analysis was performed using two-way ANOVA followed by Bonferroni *posthoc* test comparing the initial weight of their respective group

Figure 2: Tumor growth profile in LLC1 allograft model in control and REMAG treated mice

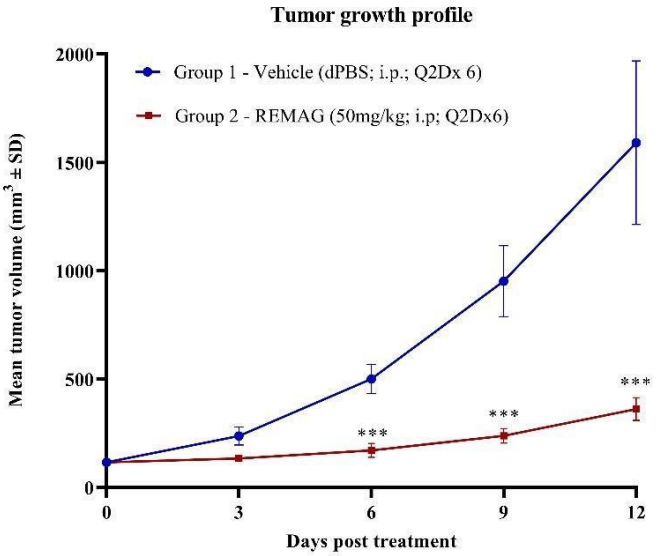

Figure 2: Mean tumor value measured at considered test days for Group 1 and 2 animals (results are expressed in Mean± SD of 6 animals in each group). ***$p < 0.001$ (t-test)

Figure 3: Real time photographs of C57BL/6 mice treated with vehicle (DPBS) and REMAG at day 12 in LLC1 tumor allograft model

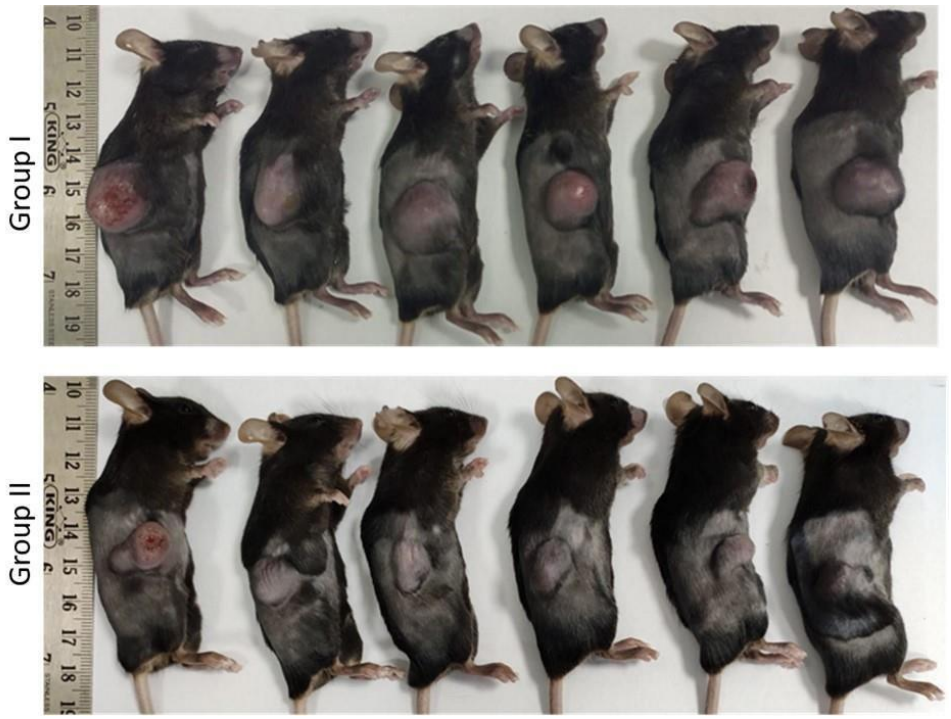

Figure 3: Real time photographs of control and REMAG treatment groups demonstrating visible tumor inhibition in REMAG treatment group when compared with control.

Figure 4: Change in % body weight of mice under in vivo LLC1 tumor allograft model

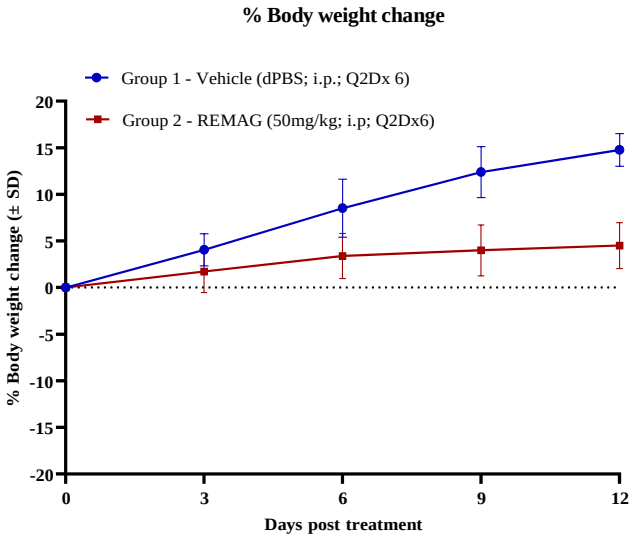

Figure 5: % body weight change during treatment period in mice bearing LLC1 tumor model. A gradual body weight increase was observed in both groups.

Table 1: Effect of REMAG treatment in tumor growth of mice bearing LLC1 tumor allograft model

Tumor volume (Mean ± SEM)					
Group/Treatment	**Day 0**	**Day 3**	**Day 6**	**Day 9**	**Day 12**
Group 1 - Vehicle (dPBS; i.p.; Q2Dx 6)	116±7	237±42	500±68	952±164	1591±378
Group 2 - REMAG (50mg/kg; i.p Q2Dx6)	116±6	133±5	171±32	238±34	361±53

Values are expressed as Mean ± SD of 6 animals in each group

Table 2: % Tumor growth inhibition (%TGI) for treated mice

% Tumor growth inhibition (%TGI)				
Group/Treatment	**Day 3**	**Day 6**	**Day 9**	**Day 12**
Group 1 - Vehicle (dPBS; i.p.; Q2Dx 6)	NA	NA	NA	NA
Group 2 - REMAG (50mg/kg; i.p Q2Dx6)	44	66	75	77

Values are expressed as Mean of 6 animals in each group

Conclusions

The study is successful in identifying the *in vivo* anti-cancer efficacy of REMAG in the LLC1 tumour allograft model, thereby making it a promising anti-cancer therapeutic candidate. Future studies are warranted to establish the anti-cancer activity of REMAG in other cancer cell lines and its molecular mechanism of actions and it would be promising to explore the specific anti-cancer mechanism.

Acknowledgements

We thankfully acknowledge Skanda Life Sciences (*In vitro* facility, Nagarbhavi, Bangalore-560098 and in vivo facility- Bidadi, Ramanagar, Bangalore- 562 109, India) for extending the *in vitro* and *in vivo* experimentation facility on outsource basis.

References

Akter, M., Sikder, M. T., Rahman, M. M., Ullah, A. A., Hossain, K. F. B., Banik, S., ... & Kurasaki, M. (2018). A systematic review on silver nanoparticles-induced cytotoxicity: Physicochemical properties and perspectives. *Journal of advanced research*, *9*, 1-16.

Banerjee, P. P., Bandyopadhyay, A., Harsha, S. N., Policegoudra, R. S., Bhattacharya, S., Karak, N., & Chattopadhyay, A. (2017). Mentha arvensis (Linn.)-mediated green silver nanoparticles trigger caspase 9-dependent cell death in MCF7 and MDA-MB-231 cells. *Breast Cancer: Targets and Therapy*, 265-278.

Chairuangkitti, P., Lawanprasert, S., Roytrakul, S., Aueviriyavit, S., Phummiratch, D., Kulthong, K., ... & Maniratanachote, R. (2013). Silver nanoparticles induce toxicity in A549 cells via ROS-dependent and ROS-independent pathways. *Toxicology in vitro*, *27*(1), 330-338.

Cho, Y. M., Mizuta, Y., Akagi, J. I., Toyoda, T., Sone, M., & Ogawa, K. (2018). Size-dependent acute toxicity of silver nanoparticles in mice. *Journal of toxicologic pathology*, *31*(1), 73-80.

Dwivedi, P., Narvi, S. S., & Tewari, R. P. (2013). Novel Scientific Appraisal of Elaeocarpus Ganitrus The Rudraksha: Nano Silver Synthesis with Aspects of Variation in Concentration Antimicrobial Activity and in Vitro Biocompatibility. *Annual Research & Review in Biology*, *4*(7), 1059-1069.

Ferlay, J., Colombet, M., Soerjomataram, I., Parkin, D. M., Piñeros, M., Znaor, A., & Bray, F. (2021). Cancer statistics for the year 2020: An overview. *International journal of cancer*, *149*(4), 778-789.

Hassanen, E. I., Khalaf, A. A., Tohamy, A. F., Mohammed, E. R., & Farroh, K. Y. (2019). Toxicopathological and immunological studies on different concentrations of chitosan-coated silver nanoparticles in rats. *International journal of nanomedicine*, 4723-4739.

Kaba, S. I., & Egorova, E. M. (2015). In vitro studies of the toxic effects of silver nanoparticles on HeLa and U937 cells. *Nanotechnology, science and applications*, 19-29.

Khorrami, S., Zarrabi, A., Khaleghi, M., Danaei, M., & Mozafari, M. R. (2018). Selective cytotoxicity of green synthesized silver nanoparticles against the MCF-7 tumor cell line and their enhanced antioxidant and antimicrobial properties. *International journal of nanomedicine*, 8013-8024.

Morais, M., Teixeira, A. L., Dias, F., Machado, V., Medeiros, R., & Prior, J. A. (2020). Cytotoxic effect of silver nanoparticles synthesized by green methods in cancer. *Journal of Medicinal Chemistry*, *63*(23), 14308-14335.

Pallela, P. N. V. K., Ummey, S., Ruddaraju, L. K., Gadi, S., Cherukuri, C. S., Barla, S., & Pammi, S. V. N. (2019). Antibacterial efficacy of green synthesized α-Fe2O3 nanoparticles using Sida cordifolia plant extract. *Heliyon*, 5(11).

Pirtarighat, S., Ghannadnia, M., & Baghshahi, S. (2019). Green synthesis of silver nanoparticles using the plant extract of Salvia spinosa grown in vitro and their antibacterial activity assessment. *Journal of Nanostructure in Chemistry*, *9*, 1-9.

Rai, D. V., Sharma, S., & Rastogi, M. (2019). Scientific research on Elaeocarpus ganitrus (Rudraksha) for its medicinal importance. *Durg V. Rai, Shiva Sharma and Manisha Rastogi*, *69*(1).

Ratan, Z. A., Haidere, M. F., Nurunnabi, M. D., Shahriar, S. M., Ahammad, A. S., Shim, Y. Y., ... & Cho, J. Y. (2020). Green chemistry synthesis of silver nanoparticles and their potential anticancer effects. *Cancers*, *12*(4), 855.

Sharma, S., Rai, D. V., & Rastogi, M. (2019). Magnetic characteristics of different Mukhi Rudraksha beads: a comparative analysis. *Int J Sci Technol Res*, *8*(11), 3329-3333.

Sharma, S., Rastogi, M., Rai, D. V., Singh, N., Sharma, G., & Singh, K. (2023). Electrical behavior of plant based material. *Materials Today: Proceedings*, *79*, 349-354.

Sharma, S., Rai, D. V., & Rastogi, M. (2021). Compositional characteristics of Rudraksha (Elaeocarpus ganitrus Roxb.). *Plant Archives (09725210)*, *21*(1).

Simon, S., Sibuyi, N. R. S., Fadaka, A. O., Meyer, S., Josephs, J., Onani, M. O., ... & Madiehe, A. M. (2022). Biomedical applications of plant extract-synthesized silver nanoparticles. *Biomedicines*, *10*(11), 2792.

Singh, J., Kumar, V., Kim, K. H., & Rawat, M. (2019). Biogenic synthesis of copper oxide nanoparticles using plant extract and its prodigious potential for photocatalytic degradation of dyes. *Environmental research*, *177*, 108569.

Sung, H., Ferlay, J., Siegel, R. L., Laversanne, M., Soerjomataram, I., Jemal, A., & Bray, F. (2021). Global cancer statistics 2020: GLOBOCAN estimates of incidence and mortality worldwide for 36 cancers in 185 countries. *CA: a cancer journal for clinicians*, 71(3), 209-249.

Wani, I. A., Ahmad, T., & Khosla, A. (2021). Recent advances in anticancer and antimicrobial activity of silver nanoparticles synthesized using phytochemicals and organic polymers. *Nanotechnology*, *32*(46), 462001.